In situ detection of the temporal and initial phase of the second harmonic of a microwave field via incoherent fluorescence

George C. Cardoso,[1] Prabhakar Pradhan,[1] Jacob Morzinski,[2] and M. S. Shahriar[1,2]
[1]*Department of Electrical and Computer Engineering, Northwestern University, Evanston, Illinois 60208, USA*
[2]*Research Laboratory of Electronics, Massachusetts Institute of Technology, Cambridge, Massachusetts 02139, USA*
(Received 26 October 2004; published 23 June 2005)

Measuring the amplitude and absolute (i.e., temporal and initial) phase of a monochromatic microwave field at a specific point of space and time has many potential applications, including precise qubit rotations and wavelength quantum teleportation. Here we show how such a measurement can indeed be made using resonant atomic probes via detection of incoherent fluorescence induced by a laser beam. This measurement is possible due to self-interference effects between the positive- and negative-frequency components of the field. In effect, the small cluster of atoms here act as a highly localized pickup coil, and the fluorescence channel acts as a transmission line.

DOI: 10.1103/PhysRevA.71.063408 PACS number(s): 32.80.Qk, 03.67.Hk, 03.67.Lx

Measurement of the amplitude and the absolute (i.e., temporal and initial) phase of a monochromatic wave is challenging because in the most general condition the spatial distribution of the field around a point is arbitrary. Therefore, one must know the impedance of the system between the point of interest and the detector, and ensure that there is no interference with the ambient field. It is recently shown in the literature that the absolute phase measurement can be used for accurate qubit rotations [1–3] and quantum wavelength teleportation [4–6].

Before we describe the physics behind this process, it is instructive to define precisely what we mean by the term "absolute phase." Consider, for example, a microwave field such that the magnetic field at a position $\boldsymbol{R}$ is given by $\boldsymbol{B}(t)=B_0\cos(\omega t+\phi)\hat{x}$, where ω is the frequency of the field and ϕ is determined simply by our choice of the origin of time. The absolute phase is the sum of the temporal and initial phases—i.e., $\omega t+\phi$. In order to illustrate how this phase can be observed directly, consider a situation where a cluster of noninteracting atoms is at rest at the same location. For simplicity, we assume each atom to be an ideal two-level system where a ground state $|0\rangle$ is coupled to an excited state $|1\rangle$ by this field $\mathbf{B}(t)$, with the atom initially in state $|0\rangle$. The Hamiltonian for this interaction is

$$\hat{H}=\varepsilon(\sigma_0-\sigma_z)/2+g(t)\sigma_x, \tag{1}$$

where $g(t)=-g_0\cos(\omega t+\phi)$, g_0 is the Rabi frequency, σ_i are the Pauli matrices, and the driving frequency $\omega=\varepsilon$ corresponds to resonant excitation. We consider g_0 to be of the form $g_0(t)=g_{0M}[1-\exp(-t/\tau_{sw})]$ with a switching time τ_{sw} relatively slow compared to other time scales in the system—i.e., $\tau_{sw}\gg\omega^{-1}$ and g_{0M}^{-1}.

As we have shown before [2,3], without the rotating-wave approximation (RWA) and to the lowest order in $\eta\equiv(g_0/4\omega)$, the amplitudes of $|0\rangle$ and $|1\rangle$ at any time t are as follows:

$$C_0(t)=\cos[g_0'(t)t/2]-2\eta\Sigma\sin[g_0'(t)t/2], \tag{2}$$

$$C_1(t)=ie^{-i(\omega t+\phi)}\{\sin[g_0'(t)t/2]+2\eta B\Sigma^*\cos[g_0'(t)t/2]\}, \tag{3}$$

where $\Sigma\equiv(i/2)\exp[-i(2\omega t+2\phi)]$ and $g_0'(t)\equiv(1/t)\int_0^t g_0(t')dt'=g_0\{1-(t/\tau_{sw})^{-1}[1-\exp(-t/\tau_{sw})]\}$. If we produce this excitation using a $\pi/2$ pulse [i.e., $g_0'(\tau)\tau=\pi/2$] and measure the population of state $|1\rangle$ after the excitation terminates (at $t=\tau$), we get a signal

$$|C_1(g_0'(\tau),\phi)|^2=1/2+\eta\sin[2(\omega\tau+\phi)]. \tag{4}$$

This signal contains information of both the amplitude and phase of the field $\boldsymbol{B}(t)$. The second term of Eq. (3) is related to the Bloch-Siegert shift [7,8], and we have called it the Bloch-Siegert oscillation (BSO) [2,3]. It is attributable to an interference between the so-called corotating and counterrotating parts of the oscillating field, with the atom acting as the nonlinear mixer. For $\eta=0$, we have the conventional Rabi flopping that is obtained with the RWA. For a stronger coupling field, where the RWA is not valid, the second term of Eq. (3) becomes important [2,3], and the population will depend now both on the Rabi frequency and the phase of the driving field. In recent years, this effect has also been observed indirectly using ultrashort optical pulses [9–11] under the name of carrier-wave Rabi flopping. However, to the best of our knowledge, the experiment we report here represents the first direct, real-time observation of this effect.

From the oscillation observed, one can infer the value of $2(\omega t+\phi)$, which represents the absolute phase of the second harmonic. This is equivalent to determine the absolute phase of the fundamental field, $(\omega t+\phi)$, modulo π. In principle, a simple modification of the experiment can be used to eliminate the modulus π uncertainty. Specifically, if one applies a dc magnetic field parallel to the rf field, it leads to a new oscillation (in the population of either level) at the fundamental frequency, with exactly the same phase as that of the driving field. In the experiment described here, we have restricted ourselves to the case of determining the absolute phase of the second harmonic only.

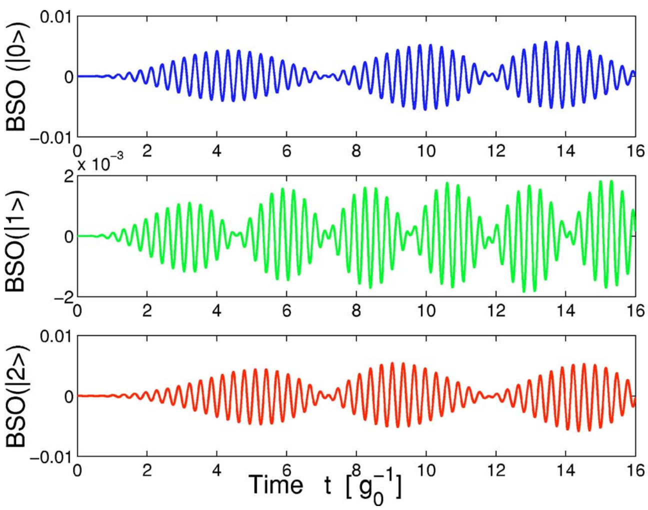

FIG. 1. BSO amplitude versus time t (in units of g_0^{-1}) plots for all the levels of a three-level system. The initial densities of the levels are $\rho_{00}(t=0)=0.5$, $\rho_{11}(t=0)=0.3$, and $\rho_{22}(t=0)=0.2$, the Rabi frequency $g_0=1$, and the resonant frequencies $\omega_{02}=\omega_{21}=10$.

While the above analytical model presented here is based on a two level system, practical examples of which are presented in Ref. [2], the effect is more generic, and is present even in three-level or multilevel systems. In particular, we employed a three-level system to observe this effect, due primarily to practical considerations. The specific system used consists of three equally spaced Zeeman sublevels of ^{87}Rb ($5\,^2S_{1/2}$: $F=1$: $m_F=-1$, 0, and 1, denoted as states $|0\rangle$, $|1\rangle$, and $|2\rangle$, respectively), where the degeneracy can be lifted by applying an external bias field. We have performed numerical simulations to confirm the presence of the BSO signature in the population dynamics of such a system as described below.

Consider an equally spaced, ladder-type three-level system ($|0\rangle$, $|1\rangle$, and $|2\rangle$). The transition frequencies for $|0\rangle$-$|1\rangle$ and $|1\rangle$-$|2\rangle$ are of the same magnitude ε. We also consider that a direct transition between $|0\rangle$ and $|2\rangle$ is not allowed. Now, let the system be pumped by the same field at a frequency ω. Consider also that the Rabi frequency for the $|0\rangle$-$|1\rangle$ transition is g_0 and that for $|1\rangle$-$|2\rangle$ is also g_0. Then, the Hamiltonian of the three-level system in a rotating frame can be written as

$$\hat{\tilde{H}}' = -g_0[1+\exp(-i2\omega t - i2\phi)](|0\rangle\langle 1| + |1\rangle\langle 2|) + \text{c.c.}, \tag{5}$$

where $\omega=\varepsilon$. The amplitudes of the three levels are calculated numerically by solving the Schrödinger equation for the above Hamiltonian. The BSO amplitudes are then calculated by subtracting the population amplitude of each level *with* the RWA from the population amplitude *without* the RWA. The BSO oscillations for all the levels of such a system are shown in Fig. 1.

The experimental configuration, illustrated schematically in Fig. 2, uses a thermal, effusive atomic beam. The rf field is applied to the atoms by a coil, and the interaction time τ is set by the time of flight of the individual atoms in the rf field before they are probed by a strongly focused and circularly polarized laser beam. The rf field couples the sublevels with $|\Delta m|=1$, as detailed in the inset of Fig. 2. Optical pumping is employed to reduce the populations of states $|1\rangle$ and $|2\rangle$ compared to that of state $|0\rangle$ prior to the interaction with the microwave field.

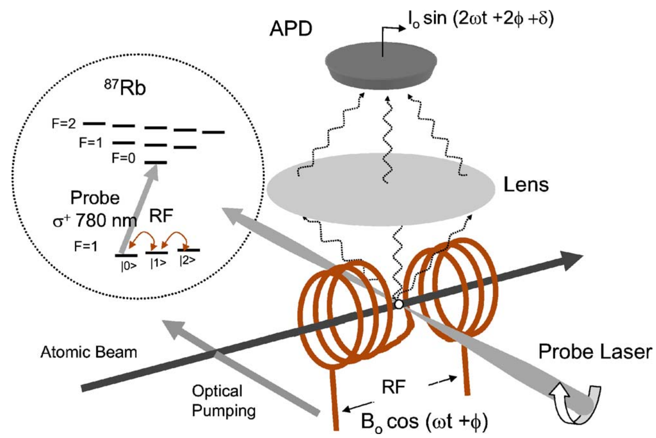

FIG. 2. Experimental setup. The 1-mm cross section rubidium atomic beam passes through the symmetry axis of the rf coil whose magnetic field is along the beam. The rf field of frequency ω is fed by a power amplifier connected to the resonant coil. A circularly polarized probe laser beam is focused down to 30 μm in diameter through a gap in the middle of the rf coil and perpendicularly to the atomic beam. The atomic fluorescence is collected by the lens and detected by an avalanche photodiode (APD). The phase signature appears in the fluorescence signal encoded in an oscillation at a frequency 2ω due to the Bloch-Siegert oscillations. In the picture, δ is an additional phase delay due to the APD circuits and cabling. Inset: Diagram of the relevant sublevels of the D_2 line of ^{87}Rb. The numbers on the left represent the total angular momentum of the respective levels. The strong driving rf field couples to the ground-state Zeeman sublevels. The probe beam must be resonant with an appropriate optical transition for the observation of the phase-locked signal, as discussed in the main text.

A given atom interacts with the rf field for a duration τ prior to excitation by the probe beam that couples state $|0\rangle$ to an excited sublevel in $5\,^2P_{3/2}$. The rf field was tuned to 0.5 MHz, with a power of about 10 W, corresponding to a Rabi frequency of about 4 MHz for the $|0\rangle\rightarrow|1\rangle$ as well as the $|1\rangle\rightarrow|2\rangle$ transition. The probe power was 0.5 mW focused to a spot of about 30 μm diameter, giving a Rabi frequency of about 60 Γ, where Γ(6.06 MHz) is the lifetime of the optical transition. The average atomic speed is 500 m/s, so that the effective pulse width of the probe, τ_{LP}, is about 60 ns, which satisfies the constraint that $\tau_{LP}\leqslant 1/\omega$. Note that the resolution of the phase measurement is essentially given by the ratio of $\min[\tau_{LP},\Gamma^{-1}]$ and $1/\omega$, and can be increased further by making the probe zone shorter. The fluorescence observed under this condition is essentially proportional to the population of level $|0\rangle$, integrated over a duration of τ_{LP}, which corresponds to less than 0.3 Rabi period of the rf driving field [for $g_{0M}/(2\pi)=4$ MHz]. Within a Rabi oscillation cycle, the BSO signal is maximum for $g_0(\tau)\tau/2=(2n+1)\pi/2$, where $n=0,1,2,\ldots$, so that there is at least one maximum of the BSO signal within the region of the probe.

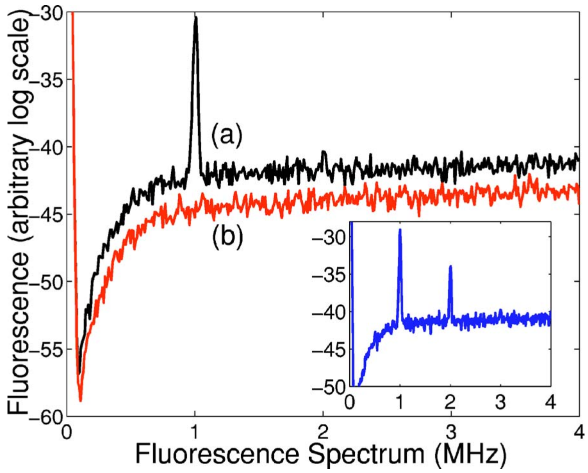

FIG. 3. Bloch-Siegert oscillation spectra. rf at 0.5 MHz and Rabi frequency around 4 MHz. (a) Probe beam resonant with the $5S_{1/2}$, $F=1 \leftrightarrow 5S_{3/2}$, $F'=0$ transition. The signal appears at 1 MHz with a linewidth less than 1 kHz (resolution limited by the spectrum analyzer). (b) Probe beam blocked. The dip structure around 100 kHz is an artifact due to the amplifier gain curve. Inset: Spectrum for same configuration and rf Rabi frequency around 10 MHz. Notice the 2-MHz harmonic which corresponds to the higher-order BSO at 4ω.

Note that atoms with different velocities have different interaction times with the rf field and produce a spread in the BSO signal amplitude within the probe region. However, *the phase of the BSO signal is the same for all the atoms*, since it corresponds to the value of $(\omega\tau+\phi)$ at the time and location of interaction. Thus, there is no washout of the BSO signal due to the velocity distribution in the atomic beam.

Figure 3 shows the spectrum of the observed BSO signal. In Fig. 3(a), we show that the BSO stays mainly at 2ω. When the probe beam is blocked, there is no signal [Fig. 3(b)]. When the rf intensity is increased a component of the BSO at 4ω begins to develop, as predicted. For the data in Fig. 4, the second harmonic of the driving field is used to trigger a 100-MHz digital oscilloscope and the fluorescence signal is averaged 256 times. When the probe beam is tuned to the $F=1 \leftrightarrow F'=0$ transition, the population at $m=-1$ state is probed. When the probe is tuned to $F=1 \leftrightarrow F'=1$, the combined populations of $m=-1$ and $m=0$ states are probed. That results in an effective detection of the complement of the population of $m=1$. On the other hand, when the probe beam is locked to the $F=1 \leftrightarrow F'=2$ transition, all three Zeeman sublevels of $F=1$ are simultaneously probed and the phase information is not clearly present, since the total population of level $F=1$ is a constant. The observed residual phase information is a result of different coupling efficiencies for each of the three ground Zeeman sublevels. We observed that the BSO signal amplitude varies as a function of an external magnetic field applied in the $\hat{z}$ direction, with a peak corresponding to a Zeeman splitting matching the applied frequency of 0.5 MHz.

In Fig. 5, we show that the fluorescence signal is phase locked to the second harmonic of the driving field. First, we placed a delay line of 0.4 μs on the cable of the reference field used to trigger the oscilloscope and recorded the fluorescence [Fig. 5(a)]. Then, we put the 0.4-μs delay line on the BSO signal cable and recorded the fluorescence [Fig. 5(b)]. The phase difference between the signals recorded in Figs. 5(a) and 5(b) is approximately 0.8 μs, as expected for a phase locked fluorescence signal. The data presented were for the probe resonant with the transition $F=1 \leftrightarrow F'=1$, but the same results were observed for $F=1 \leftrightarrow F'=0$.

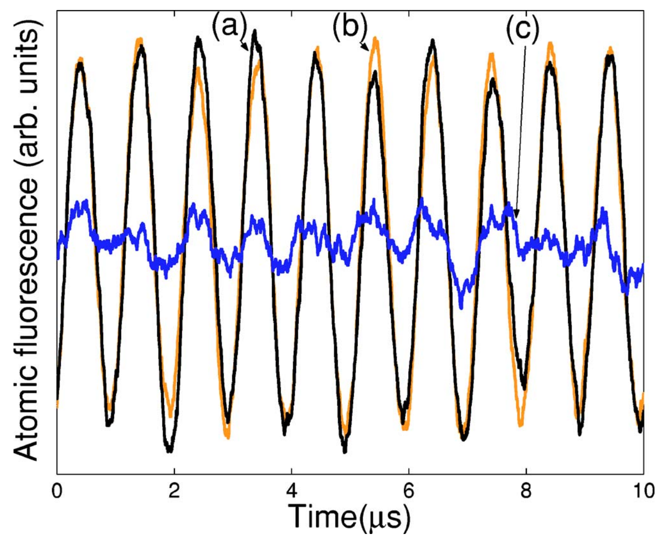

FIG. 4. Time dependence of the fluorescence signal at 2ω when the probe beam is resonant to different excited states. The lines (a), (b), and the noisy line (c) correspond to the probe locked to the transitions $F=1 \rightarrow F'=0$, $F=1 \rightarrow F'=1$, and $F=1 \rightarrow F'=2$, respectively, of the $5S_{1/2} \rightarrow 5P_{3/2}$ transition in ^{87}Rb.

To summarize, we report the first direct observation of the absolute phase of the second harmonic of an oscillating elec-

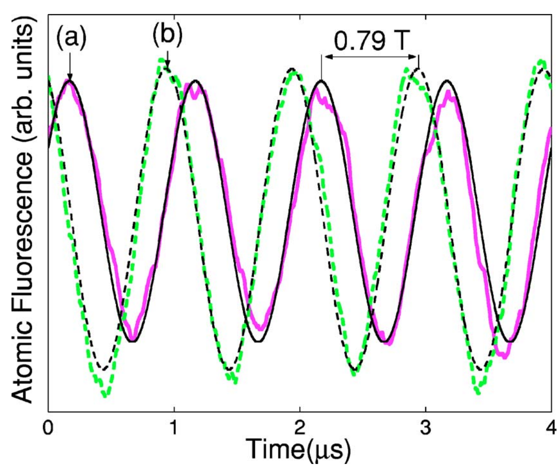

FIG. 5. Demonstration of phase-locked fluorescence. T is the period of the Bloch-Siegert oscillation. (a) Population vs time when a $0.4T$ delay line was inserted in the reference field cable. (b) Population vs time when the same $0.4T$ delay line was placed in the fluorescence signal cable. The figure shows that signal (b) is about $0.8T$ ahead of signal (a), confirming that the atomic fluorescence carries phase information which is locked to the absolute rf field phase. The solid and dashed sinusoidal smooth curves are fittings to the experimental data and were used for period and delay determination.

tromagnetic field using self-interference in an atomic resonance. This process is important in the precision of quantum bit rotations at a high speed. The knowledge of the absolute phase of a rf field at a particular point of space may also be useful for single-atom quantum optics experiments. For example, an extension of this concept may possibly be used to teleport the wavelength of an oscillator, given the presence of degenerate distant entanglement, even in the presence of unknown fluctuations in the intervening medium [4–6,12]. Finally, this localized absolute phase detector may prove useful in mapping of radio-frequency fields in microcircuits. Although a particular alkali-metal atom was used in the present experiment, the mechanism is robust and could be observed in virtually any atomic or molecular species.

This work was supported by DARPA Grant No. F30602–01–2–0546 under the QUIST program, ARO Grant No. DAAD19–001–0177 under the MURI program, NRO Grant No. NRO-000–00–C-0158, and AFOSR Grants: No. F49620–02–1-0400 and No. FA9550–04–1–0189.

[1] D. Jonathan, M. B. Plenio, and P. L. Knight, Phys. Rev. A **62**, 042307 (2000).
[2] M. S. Shahriar, P. Pradhan, and J. Morzinski, Phys. Rev. A **69**, 032308 (2004).
[3] P. Pradhan, G. C. Cardoso, and M. S. Shahriar, e-print quant-ph/0402112.
[4] R. Jozsa, D. S. Abrams, J. P. Dowling, and C. P. Williams, Phys. Rev. Lett. **85**, 2010 (2000).
[5] M. S. Shahriar, P. Pradhan, G. C. Cardoso, V. Gopal, and G. Pati, e-print quant-ph/0309085.
[6] E. Burt, C. Ekstrom, and T. Swanson, e-print quant-ph/0007030.
[7] L. Allen and J. Eberly, *Optical Resonance and Two-Level Atoms* (Wiley, New York, 1975).
[8] F. Bloch and A. J. F. Siegert, Phys. Rev. **57**, 522 (1940).
[9] G. G. Paulus *et al.*, Nature (London) **414**, 182 (2001).
[10] O. D. Mücke, T. Tritschler, M. Wegener, U. Morgner, and F. X. Kärtner, Phys. Rev. Lett. **87**, 057401 (2001).
[11] O. D. Mücke, T. Tritschler, M. Wegener, U. Morgner, and F. X. Kärtner, Phys. Rev. Lett. **89**, 127401 (2002).
[12] S. Lloyd, M. S. Shahriar, J. H. Shapiro, and P. R. Hemmer, Phys. Rev. Lett. **87**, 167903 (2001).